J Neurophysiol 106: 500–514, 2011.
First published May 4, 2011; doi:10.1152/jn.01072.2010.

Anesthetic state modulates excitability but not spectral tuning or neural discrimination in single auditory midbrain neurons

Joseph W. Schumacher,[1] David M. Schneider,[1] and Sarah M. N. Woolley[1,2]
[1]*Doctoral Program in Neurobiology and Behavior and* [2]*Department of Psychology, Columbia University, New York, New York*

Submitted 9 December 2010; accepted in final form 3 May 2011

Schumacher JW, Schneider DM, Woolley SM. Anesthetic state modulates excitability but not spectral tuning or neural discrimination in single auditory midbrain neurons. *J Neurophysiol* 106: 500–514, 2011. First published May 4, 2011; doi:10.1152/jn.01072.2010.—The majority of sensory physiology experiments have used anesthesia to facilitate the recording of neural activity. Current techniques allow researchers to study sensory function in the context of varying behavioral states. To reconcile results across multiple behavioral and anesthetic states, it is important to consider how and to what extent anesthesia plays a role in shaping neural response properties. The role of anesthesia has been the subject of much debate, but the extent to which sensory coding properties are altered by anesthesia has yet to be fully defined. In this study we asked how urethane, an anesthetic commonly used for avian and mammalian sensory physiology, affects the coding of complex communication vocalizations (songs) and simple artificial stimuli in the songbird auditory midbrain. We measured spontaneous and song-driven spike rates, spectrotemporal receptive fields, and neural discriminability from responses to songs in single auditory midbrain neurons. In the same neurons, we recorded responses to pure tone stimuli ranging in frequency and intensity. Finally, we assessed the effect of urethane on population-level representations of birdsong. Results showed that intrinsic neural excitability is significantly depressed by urethane but that spectral tuning, single neuron discriminability, and population representations of song do not differ significantly between unanesthetized and anesthetized animals.

songbird; neural encoding; anesthesia; receptive field; inferior colliculus

THE MAJORITY OF STUDIES EXAMINING cellular and systems-level processing in auditory (Knudsen and Konishi 1978; Nelken et al. 1999; Read et al. 2001; Wehr and Zador 2005; Woolley et al. 2005; Woolley et al. 2006) and visual neurons (Hubel and Wiesel 1962; Kuffler 1953; Rust et al. 2006; Weliky et al. 1996) have used anesthetized animals. Current techniques, however, allow a greater number of neurophysiological experiments to be conducted in awake animals, where neural processes involved in attention and behavior can be studied (Atiani et al. 2009; Fritz et al. 2010; Keller and Hahnloser 2009; Wang et al. 2005; Xie et al. 2007). Because current experiments and conclusions are informed by the results of previous studies and because future studies will likely be conducted using a variety of anesthetic states, it is important to determine whether and to what extent anesthesia alters neural response properties. Accordingly, the effects of anesthesia on sensory neural function have been under considerable debate (Capsius and Leppelsack 1996; Franks and Lieb 1994; Hara and Harris 2002; Sceniak and MacIver 2006; Ter-Mikaelian et al. 2007). However, few studies directly compare the complex neural coding properties of sensory neurons in anesthetized and awake animals, and even fewer include natural stimuli, which are processed differently from artificial stimuli (Rieke et al. 1995; Vinje and Gallant 2000; Woolley et al. 2006). Of those few studies, none have tested the effects of anesthesia on spectrotemporal (auditory) or spatiotemporal (visual) tuning. In the present study, we conducted a detailed comparison of the coding of communication vocalizations by auditory midbrain neurons to understand if and how anesthesia alters subcortical excitability, spectral coding, and temporal response properties.

Urethane is a common anesthetic for acute electrophysiological recordings in the sensory systems of mammals and birds. In the auditory system, urethane has been used for electrophysiology in the midbrain (LeBeau et al. 2001; Nakamoto et al. 2008; Schneider and Woolley 2010; Woolley and Casseday 2005, 2004; Woolley et al. 2005, 2006), primary forebrain (Cruikshank and Weinberger 1996; Sen et al. 2001; Wang et al. 2007; Woolley et al. 2005, 2009), higher order forebrain regions (Gentner and Margoliash 2003; Gill et al. 2008; Nishikawa and MacIver 2000; Rutkowski et al. 2002), and sensorimotor regions (Coleman et al. 2007; Margoliash 1983, 1986). Although urethane has been hypothesized to affect synaptic activity less than barbiturates (Franks and Lieb 1994; Nishikawa and MacIver 2000; Pittson et al. 2004; Scholfield 1980), it depresses spontaneous and evoked spike rates (Albrecht and Davidowa 1989; Capsius and Leppelsack 1996), leaving open the possibility that urethane influences sensory tuning. Whereas the mechanisms of urethane-induced depression have been explored at the cellular and molecular levels (Sceniak and MacIver 2006), it remains unknown to what extent stimulus coding properties are altered by urethane.

To test how the auditory encoding of complex natural and simple synthetic sounds varies depending on anesthetic state, we recorded in vivo electrophysiological responses of single auditory midbrain (avian central nucleus of the inferior colliculus, traditionally referred to as mesencephalicus lateralis pars dorsalis) neurons to songs and pure tones in urethane-anesthetized and unanesthetized zebra finches. Songbirds are model organisms for understanding the neural encoding of acoustically complex, learned communication vocalizations (Doupe and Kuhl 1999; Konishi 1989; Nottebohm 1970), and their auditory systems are well characterized (Theunissen and Shaevitz 2006). We measured spontaneous and stimulus-evoked spike rates, spectrotemporal receptive fields (STRFs), and neural discrimination from midbrain responses to conspe-

Address for reprint requests and other correspondence: S. M. N. Woolley, Columbia Univ., 406 Schermerhorn Hall, 1190 Amsterdam Ave., New York, NY 10027 (e-mail: sw2277@columbia.edu).

cific song. In the same neurons, we recorded responses to pure tone stimuli to test whether spectral tuning, stimulus thresholds, and temporal response properties were altered under urethane. Last, we compared the representations of individual songs between anesthetized and awake neuronal populations. Our results indicate that urethane depresses intrinsic neural excitability but leaves spectral tuning and neural discriminability intact in single neurons.

MATERIALS AND METHODS

All procedures were done in accordance with the NIH policies on animal care and were approved by the Columbia University Animal Care and Use Committee. Adult male zebra finches (*Taeniopygia guttata*) were either purchased from a bird farm (Canary Bird Farm, Old Bridge, NJ) or bred and raised in the Columbia University zebra finch colony. Before electrophysiological recordings were made, birds lived in a large aviary with other male zebra finches, where they received food and water ad libitum, as well as vegetables, eggs, grit, and calcium supplements.

Surgery

Two days before recordings, birds were anesthetized with a single intramuscular injection of 0.04 ml of Equithesin (0.85 g of chloral hydrate, 0.21 g of pentobarbital, 0.42 g of $MgSO_4$, 8.6 ml of propylene glycol, and 2.2 ml of 100% ethanol to a total volume of 20 ml with H_2O). After lidocaine application, feathers and skin were removed from the skull and the bird was placed in a custom-designed stereotaxic holder with its beak pointed 45 deg downward. For anesthetized recordings, small openings were made in the outer layer of the skull directly over the electrode track locations. For unanesthetized recordings, full craniotomies were made over the electrode tracks. To guide electrode placement during recordings, ink dots were applied to the skull at stereotaxic coordinates (2.7 mm lateral and 2.0 mm anterior from the bifurcation of the sagittal sinus). A small metal post was then affixed to the skull using dental acrylic, and a grounding wire was cemented in place with its end just beneath the skull, ~5 to 10 mm lateral to the junction of the midsagittal sinus. After surgery, the bird recovered for 2 days.

Stimuli

Song stimuli consisted of samples of the songs recorded from 20 different adult male zebra finches sampled at 48,828 Hz and frequency filtered between 250 and 8,000 Hz. Songs were presented from a free-field speaker at an average intensity of 72 dB SPL and in pseudorandom order for a total of 10 trials each (Fig. 1). All songs were balanced for root mean square (RMS) intensity. Songs ranged in duration between 1.62 and 2.46 s, and a silent period of 1.2–1.6 s separated the playback of subsequent songs. All songs were unfamiliar to the bird from which electrophysiological recordings were made.

Pure tone stimuli (0.5–8.0 kHz) were presented at sound levels between 20 and 90 dB SPL. Tones were 220 ms in duration, including 10-ms cosine ramps at the beginning and end. Tone stimuli were separated by silent periods of 0.4–0.5 s.

Recordings

The recording chamber was a walk-in sound attenuation booth (Industrial Acoustics). Single-neuron activity was recorded extracellularly using either tungsten microelectrodes (FHC) or glass pipettes filled with physiological saline (Sutter Instruments). For some recordings, pipette electrodes also contained 0.5% biotinylated dextran amine to mark electrode locations by iontophoretic injection. For both glass and tungsten recordings, electrode resistance was between 3 and 20 MΩ (measured at 1 kHz). Electrode signals were amplified (1,000×) and filtered (300–5,000 Hz; A-M Systems). During recording, voltage traces and action potentials were monitored using an oscilloscope (Tektronix), custom software (Python; Matlab, The MathWorks), and an audio amplifier and loudspeaker. Spike times were detected using a threshold discriminator, and spike waveforms were saved for offline sorting and analysis. For off-line sorting, spike waveforms were upsampled four times using a cubic spline function (Joshua et al. 2007). Action potentials were separated from nonspike events by waveform analyses and cluster sorting using the first three principal components of the action potential waveforms (custom software; Matlab, The MathWorks).

In preparation for anesthetized electrophysiological recordings, the bird was given three intramuscular injections of 0.03 ml of 20% urethane, separated by 20 min. All birds were wrapped in a blanket and then head-fixed in a custom stereotaxic device. For anesthetized recordings, the bird's body temperature was monitored by placing a thermometer underneath the wing and was maintained between 38 and 40°C using an electric heating pad (A-M Systems). Restrained birds were placed on a table near the center of the room, and a single speaker was located 23 cm directly in front of the bird. Neurons were recorded bilaterally and were sampled throughout the extent of the auditory midbrain, which is located ~5.5 mm ventral to the dorsal surface of the brain. Amplitude-modulated (AM) white noise was used as a search stimulus while the auditory midbrain was approached. When background multiunit activity was detected, search stimuli, including conspecific songs, modulation-limited noise, and AM white noise, were used to isolate individual neurons. We recorded from all neurons that were driven or inhibited by any of the search stimuli. Isolation was ensured by calculating the signal-to-noise ratio of action potential and nonaction potential events and by monitoring baseline spike rate throughout the recording session.

Because urethane induces a nonrecoverable anesthetic state, recordings from anesthetized birds were limited to one session per bird. Unanesthetized birds, however, were used across multiple recording sessions. This enabled us to record from more neurons in each unanesthetized bird compared with anesthetized birds. We verified that the time spent recording from each group was proportional to the number of recorded neurons by performing a linear regression of cumulative recording time and the number of recorded neurons. Recording time and data yield were highly correlated ($P < 0.0001$; $r^2 = 0.59$), indicating that the number of recorded neurons is largely determined by the time spent recording from a bird. The average cumulative recording times for individual unanesthetized and anesthetized birds were 11.25 and 7.54 h, respectively. In anesthetized birds, we referenced the recording time of each neuron to the timing of our last urethane injection (T_{rec}) and saw no relationship between the time spent under anesthesia and neural excitability. Linear regressions of T_{rec} against spontaneous spike rates ($P = 0.20$; $r^2 = 0.01$) and driven spike rates ($P = 0.43$; $r^2 = 0.01$) were not significant. This indicates that, across our recorded population of neurons from anesthetized birds, anesthesia did not alter neural activity in a time-dependent manner.

Data Analysis

Spectrotemporal receptive field estimation. We calculated STRFs by fitting a generalized linear model (GLM), a generalization of the classic linear-nonlinear-Poisson cascade model (Paninski 2004). This approach has been described previously (Calabrese et al. 2011). Briefly, the GLM describes a neuron's response as a function of the stimulus and three sets of fitted parameters: *1*) the stimulus filter, or STRF; *2*) a postspike filter that captures the dependency of the neural response on spiking history (e.g., refractoriness or burstiness); and *3*) an offset term that captures the baseline firing of the model. For each neuron, a static nonlinear

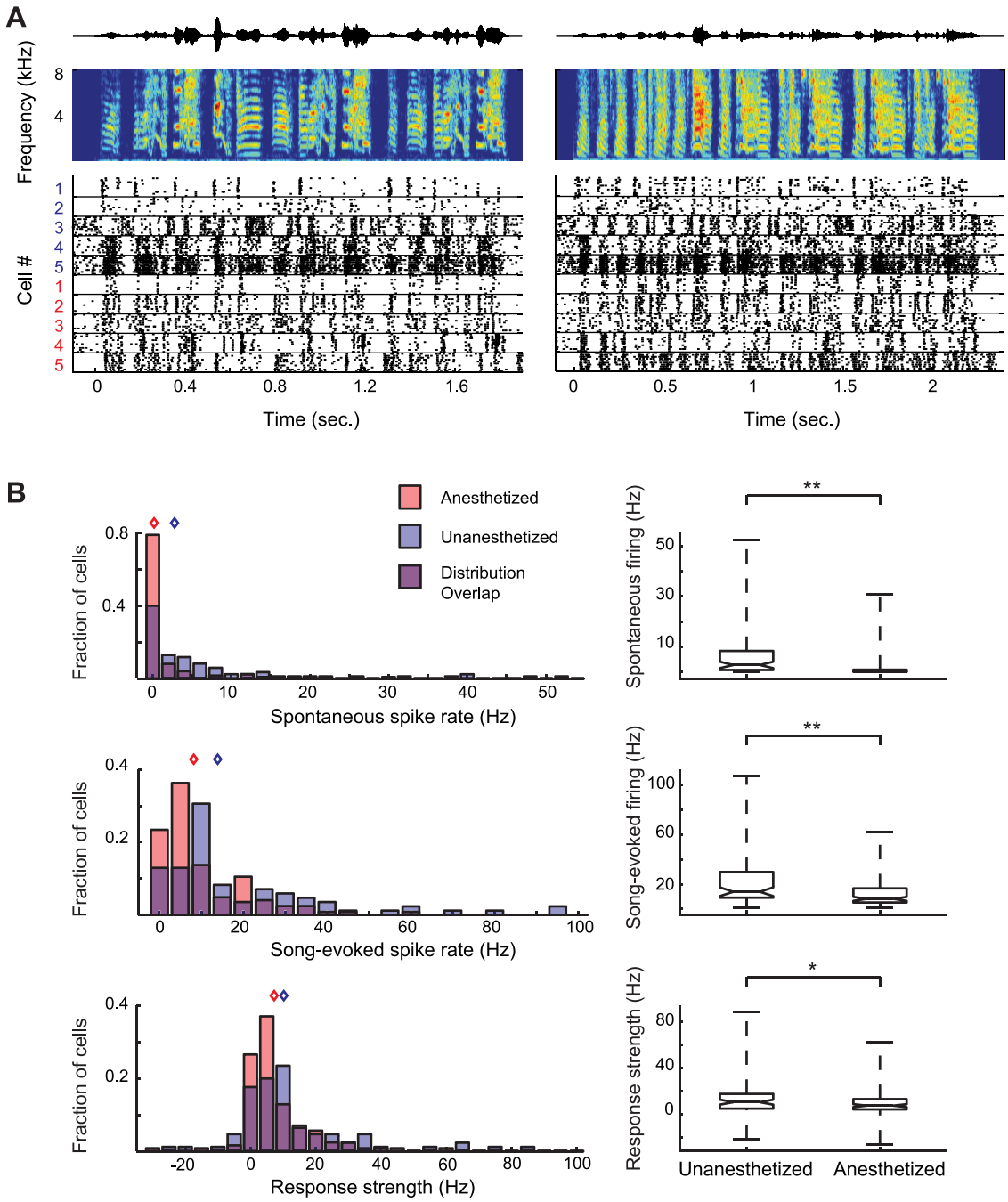

Fig. 1. Neural responses to conspecific song vary across cells and are depressed in anesthetized neurons. *A*: stimulus waveforms (*top*), song spectrograms (*middle*), and raster plots represent 10 cells' responses to 10 presentations of 2 conspecific songs. Unanesthetized (blue) and anesthetized units (red) each produced robust spiking responses and show variable levels of spontaneous and song-evoked firing. *B*: distributions and box plots of spontaneous spike rates (*top*), song-evoked spike rates (*middle*), and response strength (*bottom*) are plotted as overlapping histograms. Blue histograms indicate unanesthetized units, red histograms indicate anesthetized units, and purple areas show distribution overlaps. Blue and red diamonds indicate median values for unanesthetized and anesthetized groups, respectively. Anesthetized units ($n = 124$) had significantly lower spontaneous spike rates, song-evoked spike rates, and response strength than unanesthetized units ($n = 85$). *$P < 0.05$; **$P < 0.0001$.

function (exponential) is applied to the filtered stimulus to obtain an instantaneous spike rate (Paninski et al. 2007; Truccolo et al. 2005). To fit the model parameters, stimuli were computed as log spectrograms (Gill et al. 2006) and responses were binned at 3-ms resolution. The spectral domain of the stimulus was divided into 20 equally spaced bins, which spanned frequencies from 250 to 8,000 Hz. Model parameters were fit to the resampled stimuli and responses using custom maximum penalized likelihood algorithms (Calabrese et al. 2011).

STRF tuning measures. To compare spectrotemporal tuning under unanesthetized and anesthetized conditions, we measured four STRF tuning properties (Fig. 2) commonly used to characterize auditory neurons (Capsius and Leppelsack 1996; David et al. 2009; Escabi and Read 2003; Woolley et al. 2006): *1*) best excitatory frequency (BF), the spectral frequency that evokes the strongest neural response; *2*) excitatory spectral bandwidth (BW), the range of frequencies that are associated with an increase from mean spike rate; *3*) excitatory temporal bandwidth (tBW), the span of time over which relevant

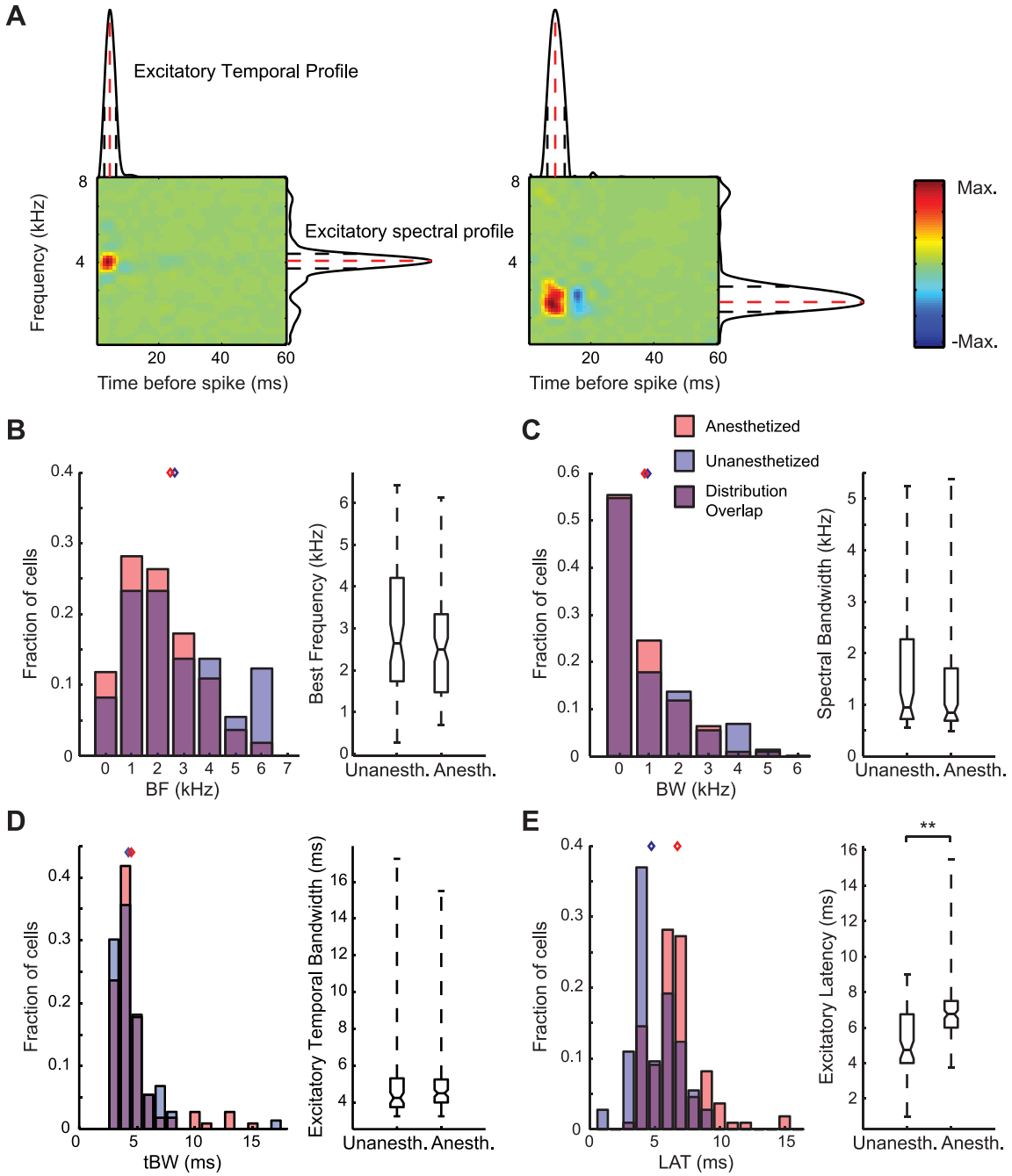

Fig. 2. Spectrotemporal receptive field (STRF) tuning properties. *A*: STRF tuning measures are plotted along the axes of representative STRFs estimated from unanesthetized (*left*) and anesthetized (*right*) responses to conspecific song. Color denotes excitatory (red) and inhibitory regions (blue) of the STRFs, normalized to the peak value of each STRF. Dashed black lines demarcate the bandwidths calculated from spectral (BW) and temporal axes (tBW). Red dashed lines illustrate the best frequency (BF) and latency to excitation (LAT) relative to the spectral and temporal axes, respectively. *B–E*: tuning parameters are displayed as overlapping histograms (unanesthetized, blue; anesthetized, red; distribution overlap, purple). Blue and red diamonds indicate median values for unanesthetized and anesthetized groups, respectively. *B*: BF. *C*: BW. *D*: tBW. *E*: LAT. LAT was shorter in unanesthetized neurons than in anesthetized neurons, indicating longer response latencies under urethane anesthesia. $^{**}P < 0.0001$. Unanesth., unanesthetized; Anesth., anesthetized.

frequencies lead to an increase from mean spike rate; and *4*) latency to excitation (LAT), the time at which relevant stimulus features excite the neuron (response latency). For the tuning measures, GLM STRFs were upsampled (3×) such that they had 1-ms temporal resolution and 60 equally spaced spectral bins from 250 to 8,000 Hz. BF was measured by setting negative STRF values to zero and averaging along the time axis. The resulting spectral tuning curve was convolved with a five-point symmetric Hanning window, and the BF was taken to be the position (Hz) of the peak of the smoothed curve. The BW was measured from the smoothed curve as the width (Hz) at half-height of the curve. The tBW was measured by setting all negative STRF values to zero and averaging along the spectral axis. The resulting temporal tuning curve was convolved with a five-point symmetric Hanning window, and the tBW was measured from the smoothed curve as the width (ms) at half-height. LAT was measured as the position (ms) of the peak of the smoothed curve.

Neurometric analysis. To quantify the ability of single neurons to discriminate among song stimuli, we implemented a *K*-means neuro-

metric that classifies spike trains into K clusters based on their proximity to one another in a high-dimensional space, where K is the number of stimuli presented (Schneider and Woolley 2010). Briefly, as with van Rossum's (2001) spike train distance metric, the K-means metric uses Euclidean distance to measure spike train similarity. Spike trains were smoothed using an exponential decay ($\tau = 10$ ms) and then iteratively clustered into K groups (Duda et al. 2001). Clusters were initially seeded with K randomly selected spike trains (1 randomly selected for each stimulus) as cluster centers. Each remaining spike train was assigned a cluster based on the seed with the closest proximity. After this initial clustering, cluster centers were recalculated as the geometric mean of the spike trains within that cluster. Spike trains were then reclustered with the new cluster centers, and this process was reiterated until a set of K clusters was converged upon. A measure of percent correct discrimination was calculated by analyzing the spike trains that belonged to each of the K clusters. Clusters were assigned a song label via a voting scheme in which each spike train in the cluster voted for the song that evoked it. Each cluster was assigned to the song that cast the most votes, and if more than one cluster had the same number of votes for a song, then the cluster with the fewest spike trains from any other song was assigned to the original song, and the other cluster was assigned to the song with the second largest spike train representation. If each cluster contained spike trains from a single song, the neuron had 100% correct discrimination. If one or more spike trains were misclassified, percent correct decreased toward chance ($100\%/K = 5\%$). The K-means neurometric was iterated 100 times. K-means was seeded with a different set of spike trains in each iteration. The resulting discrimination values are the mean performance across all 100 iterations. On a given iteration, if a spike train was equally similar to two or more templates, that spike train was scored as misclassified even if one of the templates represented the appropriate song category. We used this assignment criterion because ambiguity suggests poor discriminability.

We also calculated d' as a measure of discriminability that provided no upper bound to the estimate of a neuron's discrimination performance. To calculate d', we first smoothed each spike train with an exponential decay ($\tau = 10$ ms) and projected the spike trains from two stimuli onto a single vector that connected the average neural response for each stimulus, which is equal to the average smoothed spike train in response to that song. We then fit a normal distribution to each of the clusters and measured the d' between the clusters, which is the distance between the cluster means normalized by the variance of the clusters (Schneider and Woolley 2010). For each neuron, we calculated d' for every pair of clusters and averaged across all pairs.

As noted, each neurometric used a static decay constant τ across all neurons. The value of τ plays an important role in determining the time scale at which spiking information is available (Narayan et al. 2006; van Rossum 2001; Wang et al. 2007). Small values of τ (e.g., 1 to 10 ms) indicate that spike timing information is important for the neural discrimination of different stimuli, whereas larger values indicate that time-varying spike rate information is important for neural discrimination. We tested K-means discrimination performance over a wide range of τ values (5–100 ms) and found that the values of τ that maximized discrimination performance (τ_{opt}) in single neurons were not significantly different between neurons recorded from unanesthetized and anesthetized birds ($P = 0.19$; Mann Whitney U-test). The value of τ was set at 10 ms because the value of τ that optimized K-means discrimination in the unanesthetized and anesthetized populations (i.e., the values of τ that maximized the population averages) was ~10 ms, and because $\tau = 10$ ms has been used previously to quantify neural discrimination in songbird auditory neurons (Narayan et al. 2006; Wang et al. 2007). Furthermore, we calculated neurometric performance using a wide range of τ values and found that the specific value of $\tau = 10$ ms was not critical for our findings (see RESULTS). Because we used a relatively short value of τ, these neurometric analyses emphasized spike timing information. Previous results have shown that songbird auditory midbrain neurons do not discriminate above chance when a spike rate model of song discrimination is used (Schneider and Woolley 2010). We repeated this analysis and found that both unanesthetized and anesthetized neurons consistently failed to perform above chance when spike rate was used to discriminate among songs (data not shown).

Population analysis. We assessed neural population-level response properties under unanesthetized and anesthetized conditions by constructing neurograms and population peristimulus time histograms (pPSTHs). Each row of a neurogram consisted of the log of the time-varying PSTH of a single neuron for a single stimulus (10 trials per stimulus). Unanesthetized and anesthetized neurograms were matched for BF and contain the same number of cells (73), and neurogram rows were ordered by BF.

The pPSTHs were calculated for each song stimulus as the average PSTHs for the neural responses represented in the neurograms. For each of the unanesthetized and anesthetized neuronal populations, there were 20 pPSTHs because there were 20 song stimuli. To evaluate the degree of similarity or difference between unanesthetized and anesthetized pPSTHs for a given stimulus, we first estimated the time lag between the two by taking the cross-correlation of the unanesthetized and anesthetized pPSTHs:

$$R_{xy}(\tau) = \sum_{t=0}^{N-\tau-1} x_{t+\tau} y_t, \quad (1)$$

where x and y are, respectively, the unanesthetized and anesthetized pPSTHs during the duration of the stimulus. The time lag between x and y is then computed as the value of τ that maximizes R_{xy}. Negative time lags indicate that y lags behind x, positive time lags inidcate that x lags behind y, and a time lag equal to zero indicates no time lag. We calculated correlation coefficients between unanesthetized and anesthetized pPSTHs after correcting for the time lag between the two pPSTHs.

We assessed stimulus discriminability performance at the population level by again calculating d'. However, rather than computing d' within a single cell, we calculated stimulus discriminability by comparing the PSTHs between individual neurograms.

Frequency response area and tone tuning estimation. For a subset of the recorded neurons, we calculated frequency-response area (FRA) functions from responses to repeated presentations of pure tones ranging from 500 to 8,000 Hz (500-Hz increments) and intensities from 20 to 90 dB SPL (10-dB increments), for a total of 128 frequency-intensity combinations. These frequency-intensity ranges and increments were chosen on the basis of previous work on tone tuning in the auditory midbrain (Woolley and Casseday 2004). Frequency-intensity combinations were presented in pseudorandom order for 10 repetitions or until enough data were collected to acquire well-defined FRA plots. FRA plots depict the average response at each frequency-intensity combination.

FRAs were upsampled three times along the frequency and intensity dimensions to increase tone tuning resolution. To derive tone tuning curves from upsampled FRAs, we defined a significant excitatory response threshold as being equal to the spontaneous spike rate plus 20% of the peak driven spike rate (Sutter and Schreiner 1991). Responses to frequency-intensity combinations that met this criterion were considered to fall within the tuning curve of the neuron. We measured four response properties from the pure tone tuning curves: *1*) characteristic frequency (CF) was defined as the frequency (Hz) at which the lowest sound pressure level was necessary to evoke a significant excitatory response; *2*) BF was defined as the frequency that evoked the largest response when summed across all levels; *3*) threshold was defined as the minimum intensity to evoke a significant excitatory response; and *4*) BW was defined as the width (in Hz) of the tuning curve at 70 dB SPL, 90 dB SPL, and 20 dB above threshold.

Matching for BF. We matched unanesthetized and anesthetized units for BF for our analysis of tone tuning-response properties. First, we compared the distributions of unanesthetized and anesthetized BFs

using a Mann-Whitney *U*-test. If this test showed significantly different distributions of BFs between groups, then we used this information to remove a single data point at random from a specified bin of either the unanesthetized or anesthetized populations, depending on the disparity between the two distributions. This iterative process was repeated until the Mann-Whitney *U*-test had a nonsignificant *P* value.

Temporal response patterns. We determined temporal response patterns of individual neurons by averaging the PSTHs at the BF of the FRA at intensities that evoked a significant excitatory response. We defined the onset period of the response as the first 50 ms of the stimulus presentation, and the sustained period of the response as the second 100 ms of the stimulus presentation (modified from Wang et al. 2005). Neurons were then classified into three categories: *1*) onset neurons responded strongly at the stimulus onset but fired no or few action potentials during the sustained period; *2*) primary-like neurons fired robustly in the onset period and significantly but less during the sustained period; and *3*) sustained neurons had consistent spike rates during the onset and sustained periods.

To quantify the temporal response patterns, we used an onset index, O_{index}, defined as the onset spike rate minus the sustained spike rate, divided by the sum of the onset and sustained spike rates:

$$O_{index} = \frac{Onset_{FR} - Sustained_{FR}}{Onset_{FR} + Sustained_{FR}}, \quad (2)$$

where values could range from −1 (no onset response, significant sustained response) to 1 (significant onset response, no sustained response). O_{index} values between 0 and 1 represent a spectrum of response types from sustained ($O_{index} = 0$) to primary like ($0 < O_{index} < 1$) to onset ($O_{index} = 1$).

Spike latency. Because we observed a variety of spontaneous spike rates, the calculation of spike latency used a binless algorithm designed to discriminate between spontaneous and stimulus-evoked action potentials. This method has been described previously (Bair and Koch 1996) and has been applied to spike trains collected from inferior colliculus neurons (Chase and Young 2007). Briefly, the algorithm compares the observed spiking activity over several time windows with the activity that would be expected if the neuron were firing spontaneously with Poisson statistics. The first time at which the spiking activity significantly deviated from spontaneous Poisson activity ($P < 10^{-6}$) was considered the latency for the neuron (Bair and Koch 1996; Chase and Young 2007). In the event that the threshold was not exceeded in the first 50 ms, the latency was undefined. For each neuron, the value of the first spike latency was calculated using all significant responses, as defined in our calculation of the neuron's FRA.

RESULTS

Urethane Depresses Spike Rates

We recorded extracellular action potentials from 209 neurons. Eighty-five neurons were from 9 unanesthetized birds, and 124 neurons were from 31 anesthetized birds. We refer to birds as unanesthetized rather than "awake" because signs of wakefulness, such as eye openings and movement, varied throughout recording sessions. To measure the response properties of these neurons to complex time-varying stimuli, we recorded spike trains in response to 10 repetitions (trials) of 20 different zebra finch songs presented in pseudorandom order. Robust stimulus-locked responses were observed in both anesthetized and unanesthetized recordings (Fig. 1*A*).

To determine the effect of urethane on midbrain auditory responses to complex, natural sounds, we measured spontaneous and song-evoked spike rates during presentations of conspecific song. Anesthetized recordings yielded lower spontaneous ($P < 0.0001$, Mann-Whitney *U*-test; Fig. 1*B*, *top*) and song-evoked spike rates ($P < 0.0001$, Mann-Whitney *U*-test; Fig. 1*B*, *middle*). Response strength, defined as the evoked rate minus the spontaneous rate, was also slightly but significantly lower in anesthetized cells ($P = 0.039$, Mann-Whitney *U*-test; Fig. 1*B*, *bottom*). These results are consistent with previous studies; depression of spontaneous and stimulus-evoked spike rates has been widely reported in urethane-anesthetized preparations (Albrecht and Davidowa 1989; Capsius and Leppelsack 1996; Girman et al. 1999; Sceniak and MacIver 2006). These results indicate that, like most other systems investigated under urethane anesthesia, neural excitability is depressed in the anesthetized songbird auditory midbrain.

Effect of Urethane on Spectrotemporal Tuning During Song Coding

To determine the effects of urethane anesthesia on spectral and temporal tuning during vocal processing, we calculated STRFs from responses to 20 conspecific songs (Calabrese et al. 2011). Tuning measures were analyzed only if their GLM-predicted responses matched their actual responses with a correlation coefficient of at least 0.3 (unanesthetized: $n = 73$, 85.9%; anesthetized: $n = 111$, 89.5%). We then measured spectrotemporal tuning properties, including BF, BW, tBW, and LAT (Fig. 2*A*).

To determine whether spectral tuning to complex stimuli differed in unanesthetized and anesthetized neurons, we compared BFs and BWs between the two groups. Median values and interquartile ranges for the BF of unanesthetized and anesthetized neurons were 2.65 (1.74–4.21) and 2.48 (1.47–3.34) kHz, respectively, and did not differ ($P > 0.05$, Mann-Whitney *U*-test; Fig. 2*B*). This indicates that at the population level, midbrain auditory neurons are maximally tuned to frequencies that cover most of the range of zebra finch hearing (Okanoya and Dooling 1987) in both anesthetized and unanesthetized birds. Although BF did not differ between unanesthetized and anesthetized neurons, Fig. 2*B* shows that we recorded a larger proportion of neurons tuned to 6 kHz or higher in unanesthetized units. This is most likely due to an anatomical sampling bias; because global activity is much higher in unanesthetized birds, single-cell isolation was easiest in ventral regions where cell density is sparsest and neurons are tuned to higher frequencies (Woolley and Casseday 2004). Median values and interquartile ranges for the BW of unanesthetized and anesthetized neurons were 0.95 (0.72–2.27) and 0.85 (0.69–1.71) kHz, respectively, and were not significantly different ($P = 0.22$, Mann-Whitney *U*-test; Fig. 2*C*). These results indicate that the spectral tuning in midbrain neurons is not altered by urethane anesthesia.

Next, we asked whether temporal tuning measured from responses to song was affected by anesthetic state. Median values and interquartile ranges for unanesthetized and anesthetized tBW were 4.25 (3.75–5.31) and 4.5 (4–5.25) ms, respectively, and were not significantly different ($P = 0.52$, Mann-Whitney *U*-test; Fig. 2*D*). This suggests that the time frames over which acoustic stimuli are integrated into excitatory responses are indistinguishable for unanesthetized and anesthetized neurons. However, LAT did differ ($P < 0.0001$, Mann-Whitney *U*-test; Fig. 2*E*), indicating that unanesthetized neurons typically responded faster to the onset of excitatory

acoustic features. Median values and interquartile ranges for LAT of unanesthetized and anesthetized neurons were 4.75 (4–6.75) and 6.75 (6–7.5) ms, respectively, suggesting that intrinsic excitability was depressed in anesthetized neurons.

Urethane Does Not Affect Neural Discrimination of Songs in Single Midbrain Neurons

To quantify the ability of single neurons to discriminate among song stimuli, we used the *K*-means neurometric and computed d' for the neurons used in the STRF analysis. Median *K*-means performance values and interquartile ranges for unanesthetized and anesthetized neurons were 52.43% (22.37–90.80%) and 54.36% (25.49–98.83%), respectively, and were not significantly different ($P = 0.31$, Mann-Whitney *U*-test, Fig. 3*A*). Similar results were obtained with the d' metric, where median values and interquartile ranges for unanesthetized and anesthetized neurons were 6.71 (4.74–9.28) and 6.39 (5.08–10.18) arbitrary units (au), respectively. These distributions were not significantly different ($P = 0.75$, Mann-Whitney *U*-test; Fig. 3*B*). We tested whether the outcome of our neurometric analysis depended on the use of the static 10-ms τ (MATERIALS AND METHODS) by comparing discrimination performance with other static values of τ ranging from 1 to 50 ms. For each τ, discrimination did not differ between unanesthetized and anesthetized neurons.

We observed that d' had a strong positive correlation with song-driven spike rate in unanesthetized (linear regression: $P < 0.0001$, $r^2 = 0.63$) and anesthetized neurons (linear regression: $P < 0.0001$, $r^2 = 0.77$), but the individual "spike rate/d'" regressions had visibly different slopes (Fig. 3*C*). Although neural discrimination did not differ between the two groups, we reasoned that this change in slope could indicate differential coding efficiency between groups. Figure 3*C* shows that increases in spike rate lead to minimal gains in d' discriminability in the unanesthetized cells compared with anesthetized cells. To quantify this relationship further, we calculated a metric of neural discrimination efficiency, d'_{spike}, in which d' was normalized by driven spike rate. Median d'_{spike} values and interquartile ranges for unanesthetized and anesthetized neurons were 0.47 (0.26–0.68) and 0.72 (0.56–0.92) au, respectively, and the difference was highly significant ($P < 0.0001$, Mann-Whitney *U*-test; Fig. 3*D*). This indicates that, in the context of neural discrimination, unanesthetized neurons are less efficient than anesthetized units; the firing of action

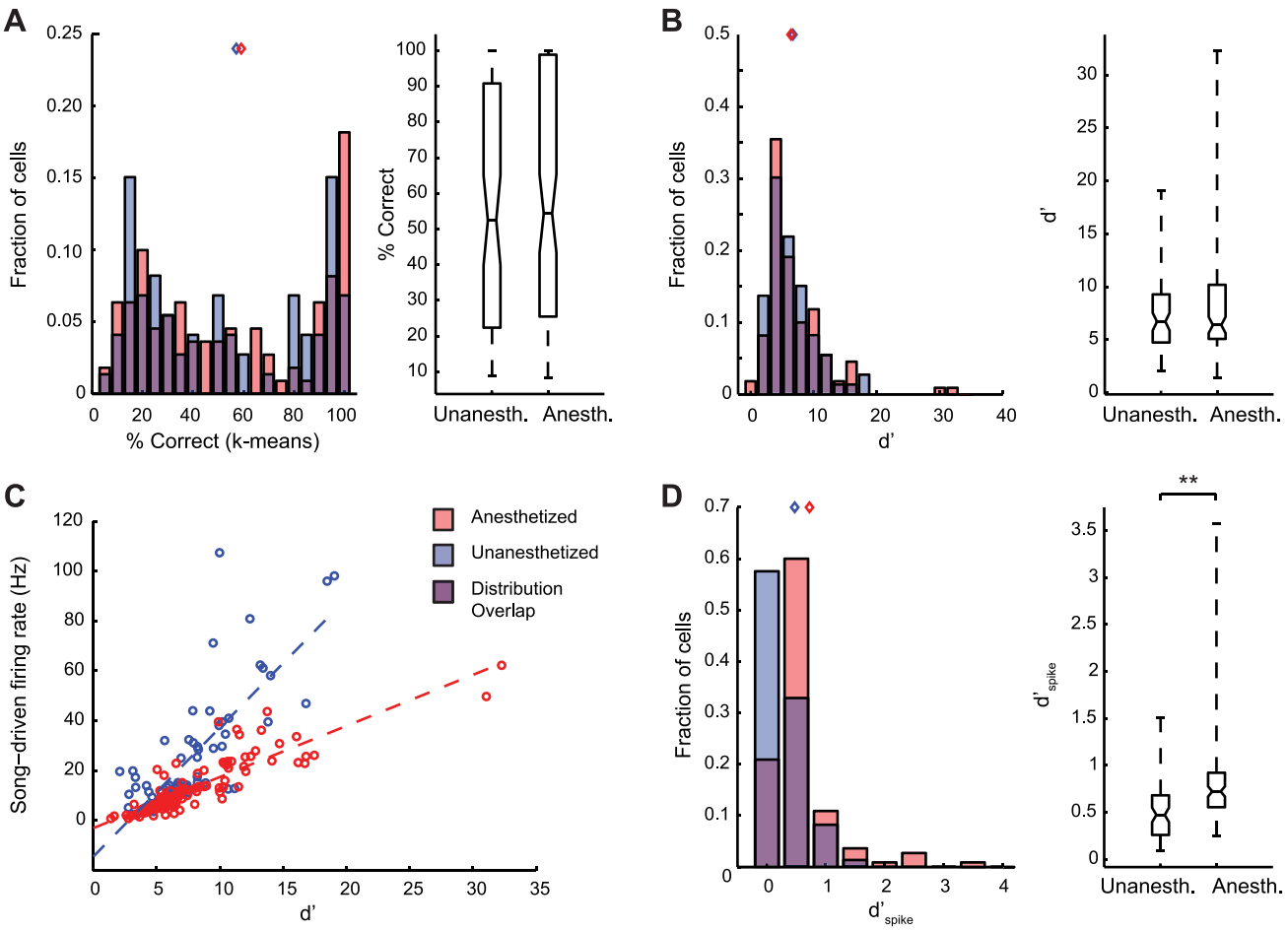

Fig. 3. Neural discriminability performance is not affected by urethane anesthesia. Distributions of performance from discriminability metrics are plotted as overlapping histograms. Blue and red diamonds indicate median values for unanesthetized and anesthetized groups, respectively. *A*: *K*-means % correct did not differ between unanesthetized and anesthetized recordings. *B*: d' values for single-neuron discriminability did not differ between unanesthetized and anesthetized recordings. *C*: the relationship between d' performance and driven spike rate was highly linear in both unanesthetized ($P < 0.0001$; $r^2 = 0.63$) and anesthetized recordings ($P < 0.0001$; $r^2 = 0.77$), but the 2 groups share different slopes with respect to this relationship. *D*: rate-normalized d' (d'_{spike}) was higher for anesthetized neurons, indicating that discriminability is more efficient under urethane anesthesia. $^{**}P < 0.0001$.

potentials is metabolically costly for a neuron, and comparable levels of spiking activity yield greater discriminability for anesthetized neurons than for unanesthetized neurons. Given our observation of depressed spontaneous spiking under anesthesia, this result is not surprising. Anesthesia may increase the threshold for excitation, and as a result, noisy spiking may occur with less frequency under anesthesia. Interestingly, despite this enhanced efficiency in anesthetized neurons, we observed no overall difference in neural discrimination performance between anesthetized and unanesthetized neurons, indicating that neural discrimination is generally robust to anesthesia-induced changes in spike rate in the auditory midbrain.

Urethane Preserves Temporal Response Patterns While Inducing a Time Lag and Enhancing Stimulus Discrimination in Neural Populations

We tested whether urethane anesthesia alters the neural representation of communication vocalizations at the population level. We computed BF- and sample size-matched neurograms and pPSTHs for unanesthetized and anesthetized populations (MATERIALS AND METHODS; Fig. 4*A*). Unanesthetized neurograms appear noisier and reflect the higher spontaneous and evoked spike rates reported above. The average temporal patterns of activation depicted by the pPSTHs were strikingly similar between the unanesthetized and anesthetized populations, but anesthetized pPSTHs showed visible time lags (Fig. 4, *B* and *C*). We computed the time lag that maximizes the correlation between unanesthetized and anesthetized pPSTHs for each stimulus using cross-correlation (MATERIALS AND METHODS). The median value of the time lag was −4 ms ($P < 0.0001$, Wilcoxon signed rank test for zero median; Fig. 4*D*). These results correspond with the shorter spike latencies observed in anesthetized STRFs (Fig. 2*E*). For each unanesthetized-anesthetized pPSTH pair, we computed the correlation coefficient, *r*, after correcting for the corresponding time lag (Fig. 4*E*). The mean lag-corrected *r* value was 0.9346 (±0.02 SD), indicating that populations of anesthetized and unanesthetized midbrain auditory neurons produce highly similar neural representations of communication vocalizations.

To quantify stimulus discriminability at the population level, we calculated the d' values between pairs of neurograms within the unanesthetized and anesthetized populations. Our method for estimating population d' was essentially identical for single-unit d', substituting single trials within a single cell with PSTHs across multiple cells. Median and interquartile range values for population d' in unanesthetized and anesthetized populations were 2.02

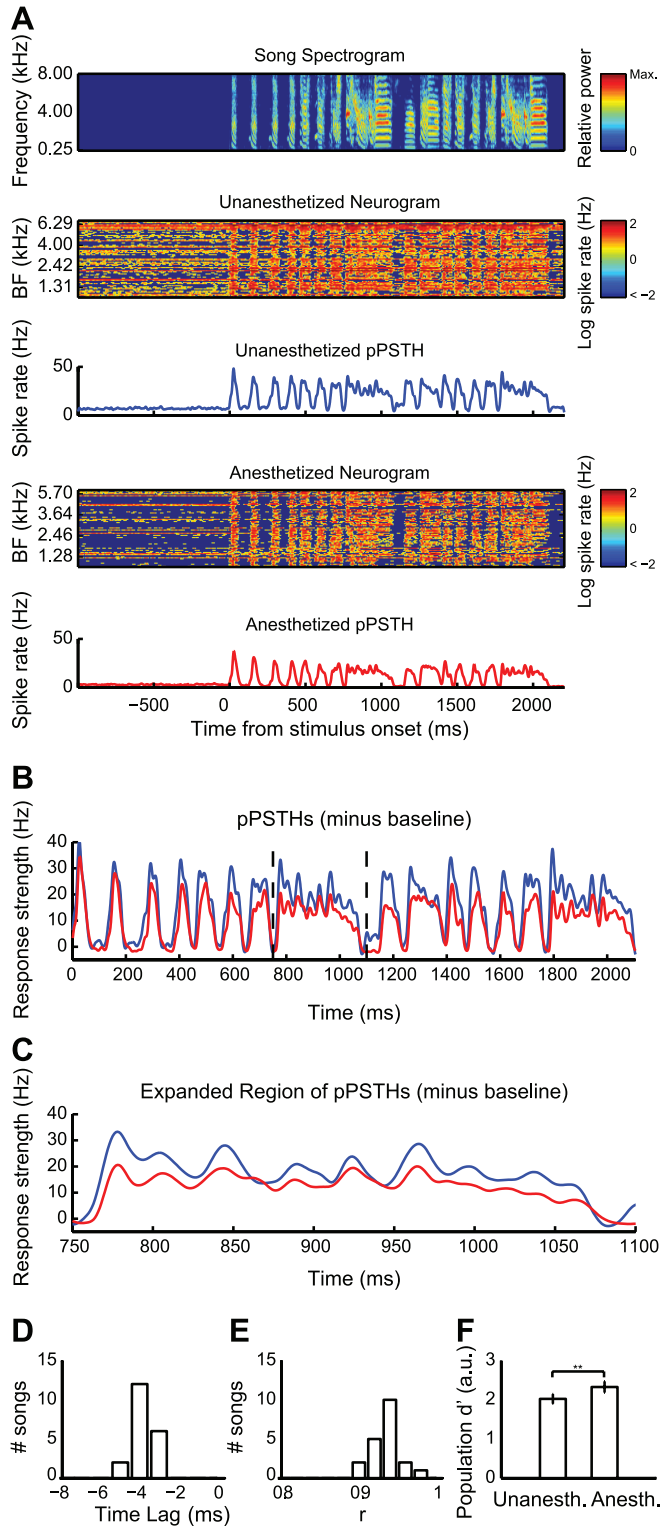

Fig. 4. Population responses are time-lagged but show conserved temporal structure under anesthesia. *A*: a sample song spectrogram (*top*; color denotes relative power) is aligned with unanesthetized and anesthetized neurograms and their corresponding population peristimulus time histograms (pPSTHs; blue and red, respectively). Each row of each neurogram represents the log of the instantaneous spike rate of an individual neuron ($n = 73$ per neurogram), arranged in order of their STRF BFs. Spontaneous and driven responses are distributed across the frequency range in both unanesthetized and anesthetized units. The unanesthetized neurogram is characterized by strong driven spiking on top of considerable noise. *B*: unanesthetized (blue) and anesthetized pPSTHs (red) for the same song shown in *A* were aligned by subtracting mean spontaneous spike rate. The red trace follows the blue trace with an apparent time lag. *C*: the region delimited by black dashed lines in *B* is expanded. *D*: the distribution of time lags corresponding to the lags in the cross-correlation of pPSTHs for the 20 song stimuli was entirely below 0 and had a median of −4 ms ($P < 0.0001$, Wilcoxon signed rank test for zero median). *E*: the distribution of lag-corrected correlation coefficients, *r*, with a mean of 0.9346 (±0.02 SD), indicates that the temporal patterns of the average neural responses to songs are highly similar in unanesthetized and anesthetized populations. *F*: median d' values for the unanesthetized population were significantly lower than in the anesthetized population, indicating that stimulus representations are more easily distinguishable in anesthetized neurons. $^{**}P < 0.0001$.

(1.94–2.12) and 2.33 (2.24–2.42) and were significantly different ($P < 0.0001$, Mann-Whitney *U*-test; Fig. 4*F*), indicating that midbrain neural discriminability is enhanced by urethane anesthesia at the population level. This seemingly contrasts with our finding that unanesthetized and anesthetized single neurons have comparable neural discriminability at the single-unit level but may indicate that aggregate neural activity in unanesthetized birds is noisier than in urethane-anesthetized birds. This is consistent with our finding of differential discrimination efficiency in single units.

Urethane Does Not Affect Spectral Bandwidth in Responses to Pure Tones

We asked whether the decreased spike rates in response to song stimuli corresponded to changes in responsiveness to simple pure tone stimuli. For a subset of neurons (65 of 85 unanesthetized and 115 of 124 anesthetized), we recorded responses to pure tones (MATERIALS AND METHODS). Responses to pure tones yielded well-defined FRAs for both unanesthetized and anesthetized midbrain neurons (Fig. 5*A*). We then used the responses to tones to measure tone tuning (Figs. 5*B* and *6*), temporal response profiles (Figs. 5*C* and 7*A*), and spike latencies (Fig. 8). Because of the known tonotopy of the songbird auditory midbrain along the dorsal-ventral axis (Woolley and Casseday 2004), the anesthetized and unanesthetized groups were first matched for BF (MATERIALS AND METHODS) to account for a potential anatomical sampling bias between the two groups. The process of matching for BF then reduced our data set to 63 unanesthetized and 91 anesthetized units.

After matching for BF across the two populations of single neurons, BF and CF (by design) did not differ between unanesthetized and anesthetized neurons ($P > 0.05$, Mann-Whitney *U*-test; Fig. 6, *A* and *B*). Medians and interquartile ranges for unanesthetized and anesthetized tone BFs were 3 (2.33–4) and 2.5 (2–3.63) Hz, respectively. Median and interquartile range values for unanesthetized and anesthetized CFs were 3 (2.33–4.17) and 2.5 (2–3.75) Hz, respectively.

BW at 20 dB above threshold did not differ between unanesthetized and anesthetized neurons ($P = 0.25$ Mann-Whitney U-test; Fig. 6*C*), with median and interquartile range values of 1 (0.83–1.67) and 1.17 (0.83–1.92) Hz, respectively. This was not dependent on the method for

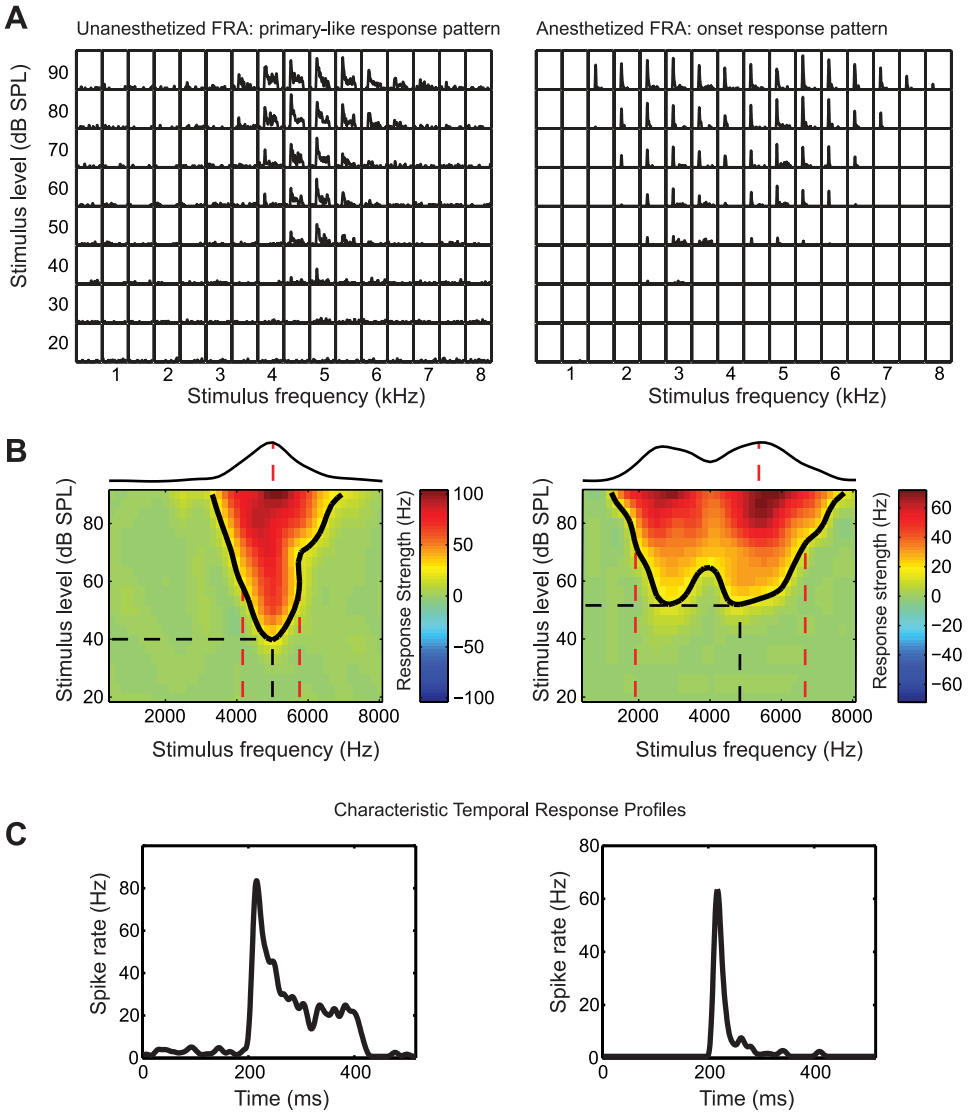

Fig. 5. Frequency-response area (FRA) tuning and temporal response profiles in single neurons. *A*: Representative FRA plots for a single unanesthetized (*left*) and a single anesthetized unit (*right*). Neurons were presented with 220 ms of pure tone stimuli at 128 frequency (0.5–8 kHz) and intensity combinations (20–90 dB SPL). *B*: FRAs were computed as color maps of response strength and were upsampled 3 times in the frequency and intensity dimensions. Black contour lines mark boundaries of significant response strengths (at least 20% of the maximum evoked spike rate, above baseline). Color map FRAs from *A* are displayed with their measured tuning properties. Characteristic frequency (CF) and intensity threshold are plotted as dashed black lines along their respective axes. BW at 20 dB above threshold is the distance between the 2 dashed red lines in the FRA. The normalized sum of the FRA along the intensity axis is above the FRA. A dashed red line at the peak along the frequency axis indicates BF. *C*: characteristic temporal response patterns of the 2 neurons were calculated as the average PSTH at BF. The unanesthetized cell had a primary-like-type response, and the anesthetized cell had an onset-type response.

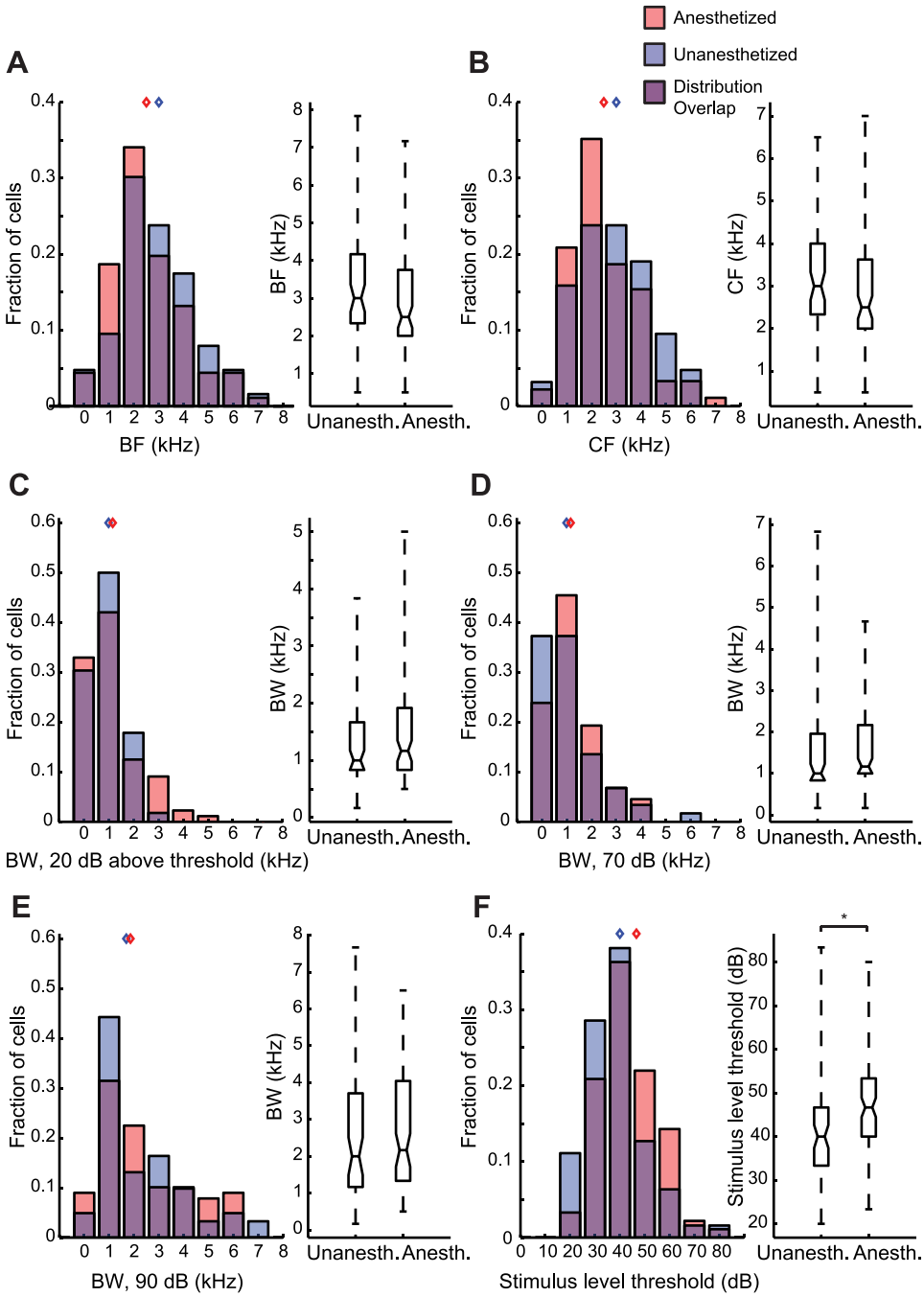

Fig. 6. Pure tone tuning properties of BF-matched samples of anesthetized ($n = 91$) and unanesthetized neurons ($n = 63$). Tuning property distributions are displayed as overlapping histograms and box plots; red histograms indicate anesthetized units, blue histograms indicate unanesthetized units, and the purple area indicates overlap in the distributions. Blue and red diamonds indicate median values for unanesthetized and anesthetized groups, respectively. *A*. BF. *B*: CF. *C*: BW at 20 dB above threshold. *D*: BW at 70 dB. E. BW at 90 dB. Tuning properties in *A–E* did not differ between unanesthetized and anesthetized units in the BF-matched samples. *F*: the average stimulus intensity threshold was lower for unanesthetized units than for anesthetized units, indicating that unanesthetized cells can respond to weaker inputs than anesthetized cells. *$P < 0.01$.

estimating BW, because BW at neither 70 ($P = 0.19$; Fig. 6*D*) nor 90 dB ($P = 0.49$; Fig. 6*E*) differed between unanesthetized or anesthetized neurons. This is consistent with our finding that the spectral BW derived from STRFs did not differ significantly between anesthetized and unanesthetized neurons. These results indicate that urethane anesthesia did not alter the ranges of tone frequencies that drive midbrain neurons to fire. Stimulus-level threshold was significantly lower in unanesthetized neurons than in anesthetized neurons ($P < 0.01$, Mann-Whitney *U*-test; Fig. 6*F*), indicating that the stimulus intensity required to drive these neurons is increased by urethane. Median and interquartile ranges for the threshold in unanesthetized and anesthetized units were 40 (33.33–46.67) and 46.67 (40–53.33) dB, respectively.

Urethane Enhances Response Onsets Relative to Sustained Firing

Consistent with previous results (Woolley and Casseday 2004), we observed a variety of temporal response patterns in unanesthetized and anesthetized neurons (Figs. 5*C* and 7*A*). We examined the temporal response patterns at BF (MATERIALS AND METHODS) to determine whether urethane alters the proportions of onset, primary-like, and sustained responses in midbrain neurons (Fig. 7*A*). Neurons that did not show a consistent response type across intensities at BF were not classified (unanesthetized, 6.2%; anesthetized, 13.2%). Of the remaining classifiable neurons, unanesthetized neurons comprised 21.3% onset responders, 46.0% primary-like responders, and 32.7%

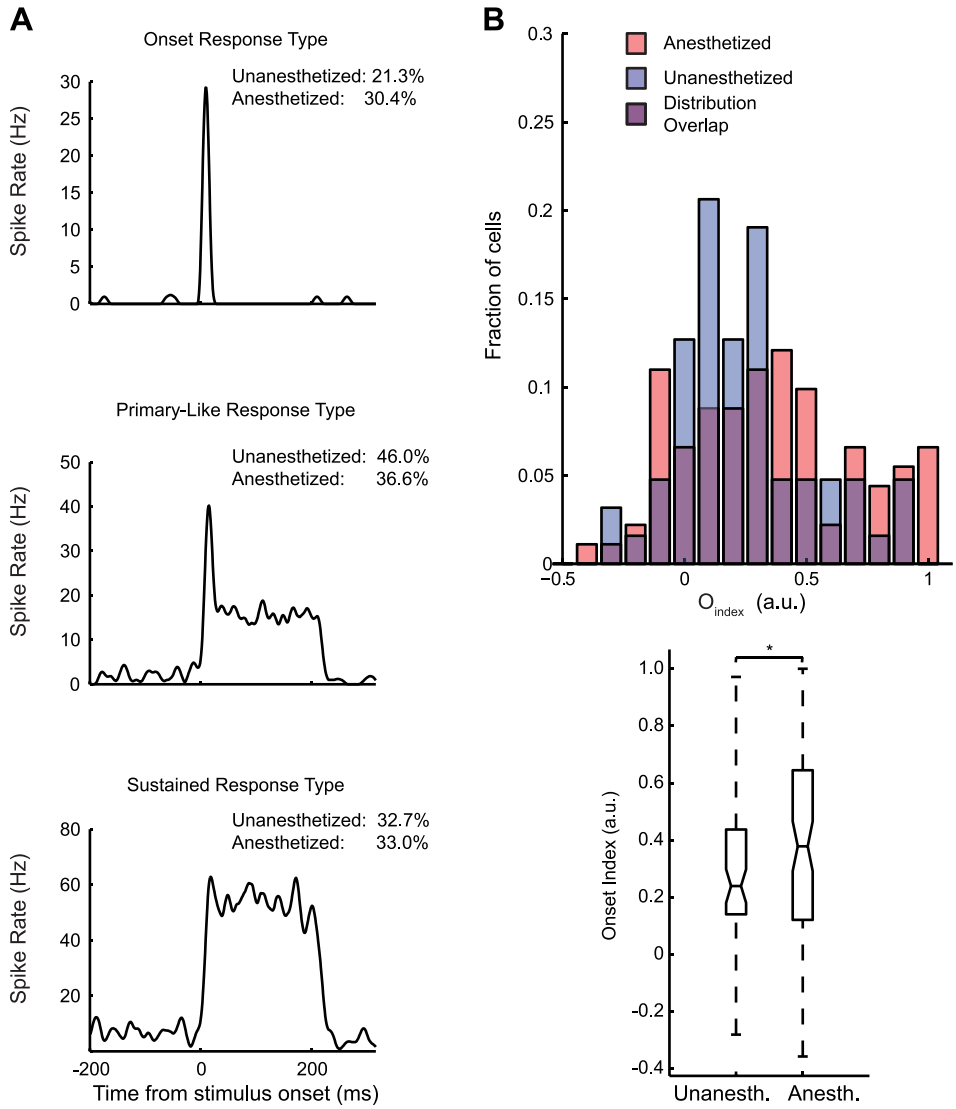

Fig. 7. Unanesthetized midbrain neurons show fewer onset-type responses than anesthetized neurons. *A*: representative examples of 3 temporal response types. Neurons that had a characteristic temporal response across intensities at BF were assigned to 1 of 3 response-type groups: onset, primary like, or sustained. Onset neurons (*top*) showed a strong onset response to pure tones, followed by little or no response. Primary-like neurons (*middle*) showed an onset response, followed by a lower sustained spiking response. Sustained neurons (*bottom*) showed a constant spike rate throughout the stimulus presentation. *B*: O_{index} (the difference divided by the sum of the first and second halves of the characteristic temporal response pattern) distributions of BF-matched samples of anesthetized and unanesthetized neurons are displayed as overlapping histograms. Blue and red diamonds indicate median values for unanesthetized and anesthetized groups, respectively. The O_{index} was typically smaller in unanesthetized neurons than in anesthetized neurons, indicating that anesthetized units have slightly more transient temporal response patterns. $*P < 0.05$.

sustained responders. Anesthetized neurons comprised 30.4% onset responders, 36.6% primary-like responders, and 33.0% sustained responders. These proportions indicate an apparent trade-off between onset and primary-like responders across anesthetic states, but sustained responders were similarly represented between the two groups.

This qualitative classification scheme is useful for capturing the tendencies of neurons to show particular response types but does not fully quantify differences among temporal response profiles. To quantify onset and sustained response characteristics, we used the onset index O_{index} as a metric for onset responsiveness (MATERIALS AND METHODS). Anesthetized neurons had significantly higher O_{index} values than unanesthetized neurons ($P < 0.05$, Mann-Whitney *U*-test), indicating that urethane enhances onset responses relative to the sustained portions of responses (Fig. 7*B*). Median and interquartile range values for O_{index} in unanesthetized and anesthetized cells were 0.24 (0.14–0.44) and 0.39 (0.12–0.65), respectively.

Urethane Increases First Spike Latency

Results showing that urethane depressed spontaneous and evoked spike rates, increased response thresholds, and enhanced onset responses suggested that urethane reduces the intrinsic excitability of auditory midbrain neurons. To further explore this possibility, we calculated the first spike latency to tone stimuli that evoked significant excitatory responses (MATERIALS AND METHODS). We hypothesized that if urethane depresses intrinsic neural excitability, then neurons should take longer to reach spike threshold in response to a given stimulus. Anesthetized neurons had significantly longer first spike latencies than unanesthetized neurons ($P < 0.01$, Mann-Whitney *U*-test; Fig. 8). Median and interquartile ranges of spike latencies for unanesthetized and anesthetized cells were 9 (7–11) and 10 (9–12) ms, respectively. This indicates that the time to reach spike threshold was slightly but significantly increased by urethane and is consistent with our observation of longer STRF latencies and a pPSTH lag in anesthetized units. Combined, these results provide strong evidence that intrinsic excitability is decreased by urethane.

DISCUSSION

Understanding the impact of anesthesia on neural coding is crucial for interpreting neurophysiological data. We compared the response properties of unanesthetized and urethane-anes-

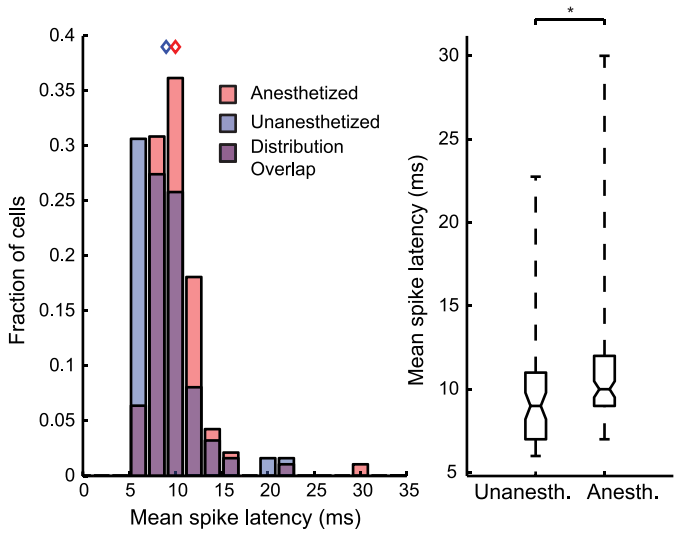

Fig. 8. Anesthesia increases spike latencies to pure tone stimuli. Average spike latencies are shown for BF-matched samples of unanesthetized and anesthetized neurons. Spike latencies were calculated for pure tone stimuli that generated response strengths that were at least 20% of the maximum song-driven spike rate. Distributions of spike latencies are depicted as overlapping histograms and box plots. Blue and red diamonds indicate median values for unanesthetized and anesthetized groups, respectively. Unanesthetized units had significantly lower spike latencies than anesthetized units. $*P < 0.01$.

thetized auditory midbrain neurons in the processing of communication vocalizations and pure tones in songbirds. Similar to previous results in other systems, we found that anesthetized neurons had significantly lower spontaneous and sound-evoked spike rates, suggesting a decrease in general excitability in anesthetized neurons. Despite decreased excitability in anesthetized neurons, we found no effects of anesthesia on spectral tuning or neural discriminability at the single-neuron level, although discrimination efficiency was higher in anesthetized neurons. This likely indicates that the higher spiking activity seen in unanesthetized neurons introduces some level of noisy spiking and that urethane anesthesia effectively reduces the "neural noise" in single cells. This is consistent with the depression of spontaneous spiking that we observed in anesthetized neurons.

Neural discrimination at the population level was sensitive to differences in spiking between unanesthetized and anesthetized neurons and was higher for anesthetized neurons. Small shifts in temporal response latency between unanesthetized and anesthetized neurons were consistent in single neurons and neuronal populations, as well as in song and tone responses. Temporal response patterns to tones also showed small, significant differences in the magnitude of response onsets relative to sustained responses. Furthermore, we observed an apparent trade-off between the proportions of onset and primary-like responders across anesthetic states, but the proportion of sustained responders was consistent in unanesthetized and anesthetized populations. Despite these differences, population representations of vocalizations were highly similar in unanesthetized and anesthetized animals, although population song discrimination was enhanced under anesthesia. These findings are consistent with a urethane-induced decrease in membrane resistance, which has been shown to be urethane's primary mechanism of action in vitro (Sceniak and MacIver 2006). Increases in membrane resistance could result in increased response latencies and intensity thresholds without inducing changes in the stimulus frequency ranges to which neurons respond. By comparing spectrotemporal tuning to complex sounds in unanesthetized and anesthetized neurons, we have shown that although intrinsic excitability may be depressed by urethane, the midbrain encoding of complex communication sounds and simple, synthetic sounds remains largely intact with urethane treatment.

An ideal data comparison would have incorporated cells in which recordings were made before and after treatment with urethane. Because of the time course of systemic urethane injections, the time required to hold a single cell under our experimental conditions would have increased approximately threefold, and complete data recordings would not have been likely. Furthermore, the irreversible effects of systemic urethane treatments preclude a washout period in which to verify neural recovery.

Effects of Anesthesia on Auditory Coding

Despite its widespread use in neurophysiology, the suitability of anesthesia for collecting neural responses to sensory stimuli has been called into question, particularly in the context of auditory processing. Others have suggested that anesthesia causes large changes in auditory response properties such as spectral tuning (Gaese and Ostwald 2001; Zurita et al. 1994), temporal response patterns (Wang et al. 2005, 2008), and temporal modulation tuning (Goldstein et al. 1959; Wang et al. 2008). For example, whereas we found comparable proportions of sustained responding neurons in unanesthetized and anesthetized neurons, Wang et al. (2005) found a prevalence of sustained responses to preferred time-varying stimuli in the auditory cortex of awake marmosets and observed that previous studies in other anesthetized animals reported primarily transient responses (deCharms and Merzenich 1996; DeWeese et al. 2003; Schnupp et al. 2001). This may have led to the conclusion that anesthesia limits what can be learned about auditory coding by significantly altering neural tuning properties away from the properties that underlie normal auditory perception. The effects of anesthesia on auditory coding depend on the brain regions that are studied, however. A recent study comparing the response properties of unanesthetized and barbiturate-anesthetized inferior colliculus (IC) and A1 neurons demonstrated that the effects of anesthesia are highly dependent on the brain area under investigation (Ter-Mikaelian et al. 2007). Pentobarbital/ketamine anesthesia decreased trial-to-trial variability in minimum spike latency in A1, and reduced response reliability. This effect was not observed in the anesthetized IC, indicating that subcortical structures may be relatively more resistant to anesthesia than cortex. Thus concerns regarding the use of anesthetized preparations should depend on the neural population under investigation. Although our study did not compare the influence of anesthesia in forebrain and midbrain neurons, we also found that a diversity of midbrain response properties are surprisingly stable regardless of anesthetic state; spectral tuning, neural song discrimination, and the temporal response patterns evoked by songs were not altered by urethane in single neurons. However, we cannot rule out the possibility that auditory coding properties relating to other classes of sensory stimuli, such as spatial location or phase sensitivity, are altered by urethane.

Because different anesthetics have different mechanisms of action, some are likely to have larger effects on sensory responses than others. The studies that have shown large effects of anesthesia on auditory coding used barbiturates and frequently used ketamine. For example, Gaese and Ostwald (2001) showed that Equithesin entirely eliminated responses to pure tones in a majority of A1 neurons, but cells that still had well-defined tone responses under anesthesia showed a decrease in tuning curve sharpness. Zurita et al. (1994) found that ketamine and pentobarbital treatment led to changes in tone tuning bandwidth in a subset of A1 and thalamic recordings. We did not observe changes in frequency bandwidths in STRFs or in pure tone tuning curves. This difference may be explained by the use of different anesthetics. Barbiturates alter the kinetics of synaptic transmission. For example, pentobarbital lengthens the open time of GABA-mediated chloride channels (Macdonald et al. 1989; Nicoll et al. 1975). Ketamine is a noncompetitive NMDA antagonist (Franks and Lieb 1994) and reduces AMPA-mediated depolarization (Leong et al. 2004; Ter-Mikaelian et al. 2007). These effects are not observed under other anesthetics, such as urethane. Sceniak and McIver (2006) demonstrated that urethane induced depressions in spike rate by decreasing membrane input resistance in neurons in vitro. Changes in membrane resistance were caused by an increase in tonic background K^+ conductance, mediated specifically by the selective opening of Ba^{2+}-sensitive K^+ leak currents, and no influence on excitatory or inhibitory synaptic transmission was found using relevant concentrations of urethane. Because anesthesia is advantageous for some intracellular and long-duration recordings and is important for maintaining consistent behavioral states in some experiments, eliminating anesthesia is not feasible for many in neurophysiology studies. The irreversible effects of urethane force experiments to be terminal and therefore cannot be used if repeated recording sessions are required over multiple days from a single animal. In other cases, urethane is advantageous for sensory coding studies that require anesthesia because it affects auditory coding less than do other anesthetics.

Comparisons to Previous Auditory Coding Studies Using Urethane

The effects of urethane anesthesia on vocalization coding may be species dependent. Consistent with our findings, Capsius and Leppelsack (1996) observed substantial urethane-induced changes in spike rate and spike latency in subregions of the starling primary auditory forebrain (avian homolog of A1). Narayan et al. (2006) found no differences in neural discriminability performance among urethane-anesthetized and unanesthetized responses to songs in zebra finch primary forebrain neurons. However, Huetz et al. (2009) found that spike-timing reliability was higher in unanesthetized than in anesthetized neurons in responses of guinea pig thalamic and cortical neurons to vocalizations. Because spike timing reliability and neural discriminability are comparable measures, our finding that unanesthetized and anesthetized neurons show similar levels of neural discriminability appears contrary to their findings. The differences between the findings of Huetz et al. (2009) and those from songbird studies may be attributable to species differences.

The use of urethane anesthesia has played an important role in studies on vocal learning and sensorimotor integration in songbirds. Urethane-anesthetized neural recordings in the vocal control nuclei HVC and RA show response selectivity for a bird's own song (BOS), compared with conspecific song or reversed BOS (Dave et al. 1998; Doupe and Konishi 1991; Lewicki 1996; Margoliash 1983, 1986; Margoliash and Fortune 1992). However, this BOS selectivity is suppressed when birds are awake (Schmidt and Konishi 1998). The gating of HVC BOS responses by behavioral state is mediated by the release of norepinephrine in the sensorimotor nucleus NIf, which is high in awake conditions and low in anesthetized or sedated conditions (Cardin and Schmidt 2003, 2004a, 2004b). This implicates attentional mechanisms in mediating the flow of auditory information into the song system. Because the representation of auditory information is stable across anesthetic states in the songbird auditory midbrain, it is not likely that such attentional mechanisms would be triggered by changes in neural activity at the level of the midbrain or lower brain stem, implicating higher order regions in the triggering of attention to gate the flow of auditory information to the song system.

Conclusions

Our results are consistent with previous studies suggesting that urethane decreases the intrinsic excitability of sensory neurons through changes in membrane electrical properties and that, compared with other anesthetics, urethane has minimal effects on synaptic transmission. Despite significant changes in spike rates and response latencies under urethane anesthesia, single-neuron spectral tuning and neural discriminability performance were not affected. Although our results suggest stability across anesthetic states at the level of the midbrain, we cannot rule out more pronounced sensitivity to anesthesia in higher brain regions, such as that which is known to occur in the songbird HVC. Our results indicate that urethane is suitable for studying complex auditory response properties, but important considerations must be made when comparing results from studies using different species, stimuli, anesthetics, and brain regions.

ACKNOWLEDGMENTS

We thank Brandon Warren for developing the software used to collect electrophysiological data and for technical support. We thank Ana Calabrese and Liam Paninski for helpful discussions and their work on the GLM.

GRANTS

This work is supported by National Institutes of Health Grants F31-DC010301 (D. M. Schneider), R01-DC009810 (S. M. N. Woolley), and T32-NS64928-1 (J. W. Schumacher) and National Science Foundation Grant IOS-0920081 (S. M. N. Woolley).

DISCLOSURES

No conflicts of interest, financial or otherwise, are declared by the author(s).

REFERENCES

Albrecht D, Davidowa H. Action of urethane on dorsal lateral geniculate neurons. *Brain Res Bull* 22: 923–927, 1989.

Atiani S, Elhilali M, David SV, Fritz JB, Shamma SA. Task difficulty and performance induce diverse adaptive patterns in gain and shape of primary auditory cortical receptive fields. *Neuron* 61: 467–480, 2009.

Bair W, Koch C. Temporal precision of spike trains in extrastriate cortex of the behaving macaque monkey. *Neural Comput* 8: 1185–1202, 1996.

Calabrese A, Schumacher JW, Schneider DM, Paninski L, Woolley SM. A generalized linear model for estimating spectrotemporal receptive fields from responses to natural sounds. *PLoS One* 6: e16104, 2011.

Capsius B, Leppelsack HJ. Influence of urethane anesthesia on neural processing in the auditory cortex analogue of a songbird. *Hear Res* 96: 59–70, 1996.

Cardin JA, Schmidt MF. Song system auditory responses are stable and highly tuned during sedation, rapidly modulated and unselective during wakefulness, and suppressed by arousal. *J Neurophysiol* 90: 2884–2899, 2003.

Cardin JA, Schmidt MF. Auditory responses in multiple sensorimotor song system nuclei are co-modulated by behavioral state. *J Neurophysiol* 91: 2148–2163, 2004a.

Cardin JA, Schmidt MF. Noradrenergic inputs mediate state dependence of auditory responses in the avian song system. *J Neurosci* 24: 7745–7753, 2004b.

Chase SM, Young ED. First-spike latency information in single neurons increases when referenced to population onset. *Proc Natl Acad Sci USA* 104: 5175–5180, 2007.

Coleman MJ, Roy A, Wild JM, Mooney R. Thalamic gating of auditory responses in telencephalic song control nuclei. *J Neurosci* 27: 10024–10036, 2007.

Cruikshank SJ, Weinberger NM. Receptive-field plasticity in the adult auditory cortex induced by Hebbian covariance. *J Neurosci* 16: 861–875, 1996.

Dave AS, Yu AC, Margoliash D. Behavioral state modulation of auditory activity in a vocal motor system. *Science* 282: 2250–2254, 1998.

David SV, Mesgarani N, Fritz JB, Shamma SA. Rapid synaptic depression explains nonlinear modulation of spectro-temporal tuning in primary auditory cortex by natural stimuli. *J Neurosci* 29: 3374–3386, 2009.

deCharms RC, Merzenich MM. Primary cortical representation of sounds by the coordination of action-potential timing. *Nature* 381: 610–613, 1996.

DeWeese MR, Wehr M, Zador AM. Binary spiking in auditory cortex. *J Neurosci* 23: 7940–7949, 2003.

Doupe AJ, Konishi M. Song-selective auditory circuits in the vocal control system of the zebra finch. *Proc Natl Acad Sci USA* 88: 11339–11343, 1991.

Doupe AJ, Kuhl PK. Birdsong and human speech: common themes and mechanisms. *Annu Rev Neurosci* 22: 567–631, 1999.

Duda RO, Hart PE, Stork DG. *Pattern Classification*. New York: Wiley, 2001.

Escabi MA, Read HL. Representation of spectrotemporal sound information in the ascending auditory pathway. *Biol Cybern* 89: 350–362, 2003.

Franks NP, Lieb WR. Molecular and cellular mechanisms of general anaesthesia. *Nature* 367: 607–614, 1994.

Fritz JB, David SV, Radtke-Schuller S, Yin P, Shamma SA. Adaptive, behaviorally gated, persistent encoding of task-relevant auditory information in ferret frontal cortex. *Nat Neurosci* 13: 1011–1019, 2010.

Gaese BH, Ostwald J. Anesthesia changes frequency tuning of neurons in the rat primary auditory cortex. *J Neurophysiol* 86: 1062–1066, 2001.

Gentner TQ, Margoliash D. Neuronal populations and single cells representing learned auditory objects. *Nature* 424: 669–674, 2003.

Gill P, Woolley SM, Fremouw T, Theunissen FE. What's that sound? Auditory area CLM encodes stimulus surprise, not intensity or intensity changes. *J Neurophysiol* 99: 2809–2820, 2008.

Gill P, Zhang J, Woolley SM, Fremouw T, Theunissen FE. Sound representation methods for spectro-temporal receptive field estimation. *J Comput Neurosci* 21: 5–20, 2006.

Girman SV, Sauve Y, Lund RD. Receptive field properties of single neurons in rat primary visual cortex. *J Neurophysiol* 82: 301–311, 1999.

Goldstein MH, Kiang NYS, Brown RM. Responses of the auditory cortex to repetitive acoustic stimuli. *J Acoust Soc Am* 31: 356–364, 1959.

Hara K, Harris RA. The anesthetic mechanism of urethane: the effects on neurotransmitter-gated ion channels. *Anesth Analg* 94: 313–318, 2002.

Hubel DH, Wiesel TN. Receptive fields, binocular interaction and functional architecture in the cat's visual cortex. *J Physiol* 160: 106–154, 1962.

Huetz C, Philibert B, Edeline JM. A spike-timing code for discriminating conspecific vocalizations in the thalamocortical system of anesthetized and awake guinea pigs. *J Neurosci* 29: 334–350, 2009.

Joshua M, Elias S, Levine O, Bergman H. Quantifying the isolation quality of extracellularly recorded action potentials. *J Neurosci Methods* 163: 267–282, 2007.

Keller GB, Hahnloser RH. Neural processing of auditory feedback during vocal practice in a songbird. *Nature* 457: 187–190, 2009.

Knudsen EI, Konishi M. A neural map of auditory space in the owl. *Science* 200: 795–797, 1978.

Konishi M. Birdsong for neurobiologists. *Neuron* 3: 541–549, 1989.

Kuffler SW. Discharge patterns and functional organization of mammalian retina. *J Neurophysiol* 16: 37–68, 1953.

LeBeau FE, Malmierca MS, Rees A. Iontophoresis in vivo demonstrates a key role for $GABA_A$ and glycinergic inhibition in shaping frequency response areas in the inferior colliculus of guinea pig. *J Neurosci* 21: 7303–7312, 2001.

Leong D, Puil E, Schwarz D. Ketamine blocks non-*N*-methyl-D-aspartate receptor channels attenuating glutamatergic transmission in the auditory cortex. *Acta Otolaryngol* 124: 454–458, 2004.

Lewicki MS. Intracellular characterization of song-specific neurons in the zebra finch auditory forebrain. *J Neurosci* 16: 5855–5863, 1996.

Macdonald RL, Rogers CJ, Twyman RE. Barbiturate regulation of kinetic-properties of the $GABA_A$ receptor channel of mouse spinal neurons in culture. *J Physiol* 417: 483–500, 1989.

Margoliash D. Acoustic parameters underlying the responses of song-specific neurons in the white-crowned sparrow. *J Neurosci* 3: 1039–1057, 1983.

Margoliash D. Preference for autogenous song by auditory neurons in a song system nucleus of the white-crowned sparrow. *J Neurosci* 6: 1643–1661, 1986.

Margoliash D, Fortune ES. Temporal and harmonic combination-sensitive neurons in the zebra finch's HVc. *J Neurosci* 12: 4309–4326, 1992.

Nakamoto KT, Jones SJ, Palmer AR. Descending projections from auditory cortex modulate sensitivity in the midbrain to cues for spatial position. *J Neurophysiol* 99: 2347–2356, 2008.

Narayan R, Grana G, Sen K. Distinct time scales in cortical discrimination of natural sounds in songbirds. *J Neurophysiol* 96: 252–258, 2006.

Nelken I, Rotman Y, Bar Yosef O. Responses of auditory-cortex neurons to structural features of natural sounds. *Nature* 397: 154–157, 1999.

Nicoll RA, Eccles JC, Oshima T, Rubia F. Prolongation of hippocampal inhibitory postsynaptic potentials by barbiturates. *Nature* 258: 625–627, 1975.

Nishikawa K, MacIver MB. Membrane and synaptic actions of halothane on rat hippocampal pyramidal neurons and inhibitory interneurons. *J Neurosci* 20: 5915–5923, 2000.

Nottebohm F. Ontogeny of bird song. *Science* 167: 950–956, 1970.

Okanoya K, Dooling RJ. Hearing in passerine and psittacine birds: a comparative study of absolute and masked auditory thresholds. *J Comp Psychol* 101: 7–15, 1987.

Paninski L. Maximum likelihood estimation of cascade point-process neural encoding models. *Network* 15: 243–262, 2004.

Paninski L, Pillow J, Lewi J. Statistical models for neural encoding, decoding, and optimal stimulus design. *Prog Brain Res* 165: 493–507, 2007.

Pittson S, Himmel AM, MacIver MB. Multiple synaptic and membrane sites of anesthetic action in the CA1 region of rat hippocampal slices. *BMC Neurosci* 5: 52, 2004.

Read HL, Winer JA, Schreiner CE. Modular organization of intrinsic connections associated with spectral tuning in cat auditory cortex. *Proc Natl Acad Sci USA* 98: 8042–8047, 2001.

Rieke F, Bodnar DA, Bialek W. Naturalistic stimuli increase the rate and efficiency of information transmission by primary auditory afferents. *Proc Biol Sci* 262: 259–265, 1995.

Rust NC, Mante V, Simoncelli EP, Movshon JA. How MT cells analyze the motion of visual patterns. *Nat Neurosci* 9: 1421–1431, 2006.

Rutkowski RG, Shackleton TM, Schnupp JW, Wallace MN, Palmer AR. Spectrotemporal receptive field properties of single units in the primary, dorsocaudal and ventrorostral auditory cortex of the guinea pig. *Audiol Neurootol* 7: 214–227, 2002.

Sceniak MP, MacIver MB. Cellular actions of urethane on rat visual cortical neurons in vitro. *J Neurophysiol* 95: 3865–3874, 2006.

Schmidt MF, Konishi M. Gating of auditory responses in the vocal control system of awake songbirds. *Nat Neurosci* 1: 513–518, 1998.

Schneider DM, Woolley SM. Discrimination of communication vocalizations by single neurons and groups of neurons in the auditory midbrain. *J Neurophysiol* 103: 3248–3265, 2010.

Schnupp JW, Mrsic-Flogel TD, King AJ. Linear processing of spatial cues in primary auditory cortex. *Nature* 414: 200–204, 2001.

Scholfield CN. Potentiation of inhibition by general anaesthetics in neurones of the olfactory cortex in vitro. *Pflügers Arch* 383: 249–255, 1980.

Sen K, Theunissen FE, Doupe AJ. Feature analysis of natural sounds in the songbird auditory forebrain. *J Neurophysiol* 86: 1445–1458, 2001.

Sutter ML, Schreiner CE. Physiology and topography of neurons with multipeaked tuning curves in cat primary auditory cortex. *J Neurophysiol* 65: 1207–1226, 1991.

Ter-Mikaelian M, Sanes DH, Semple MN. Transformation of temporal properties between auditory midbrain and cortex in the awake Mongolian gerbil. *J Neurosci* 27: 6091–6102, 2007.

Theunissen FE, Shaevitz SS. Auditory processing of vocal sounds in birds. *Curr Opin Neurobiol* 16: 400–407, 2006.

Truccolo W, Eden UT, Fellows MR, Donoghue JP, Brown EN. A point process framework for relating neural spiking activity to spiking history, neural ensemble, and extrinsic covariate effects. *J Neurophysiol* 93: 1074–1089, 2005.

van Rossum MC. A novel spike distance. *Neural Comput* 13: 751–763, 2001.

Vinje WE, Gallant JL. Sparse coding and decorrelation in primary visual cortex during natural vision. *Science* 287: 1273–1276, 2000.

Wang L, Narayan R, Grana G, Shamir M, Sen K. Cortical discrimination of complex natural stimuli: can single neurons match behavior? *J Neurosci* 27: 582–589, 2007.

Wang X, Lu T, Bendor D, Bartlett E. Neural coding of temporal information in auditory thalamus and cortex. *Neuroscience* 157: 484–494, 2008.

Wang X, Lu T, Snider RK, Liang L. Sustained firing in auditory cortex evoked by preferred stimuli. *Nature* 435: 341–346, 2005.

Wehr M, Zador AM. Synaptic mechanisms of forward suppression in rat auditory cortex. *Neuron* 47: 437–445, 2005.

Weliky M, Bosking WH, Fitzpatrick D. A systematic map of direction preference in primary visual cortex. *Nature* 379: 725–728, 1996.

Woolley SM, Casseday JH. Processing of modulated sounds in the zebra finch auditory midbrain: responses to noise, frequency sweeps, and sinusoidal amplitude modulations. *J Neurophysiol* 94: 1143–1157, 2005.

Woolley SM, Casseday JH. Response properties of single neurons in the zebra finch auditory midbrain: response patterns, frequency coding, intensity coding, and spike latencies. *J Neurophysiol* 91: 136–151, 2004.

Woolley SM, Fremouw TE, Hsu A, Theunissen FE. Tuning for spectro-temporal modulations as a mechanism for auditory discrimination of natural sounds. *Nat Neurosci* 8: 1371–1379, 2005.

Woolley SM, Gill PR, Fremouw T, Theunissen FE. Functional groups in the avian auditory system. *J Neurosci* 29: 2780–2793, 2009.

Woolley SM, Gill PR, Theunissen FE. Stimulus-dependent auditory tuning results in synchronous population coding of vocalizations in the songbird midbrain. *J Neurosci* 26: 2499–2512, 2006.

Xie R, Gittelman JX, Pollak GD. Rethinking tuning: in vivo whole-cell recordings of the inferior colliculus in awake bats. *J Neurosci* 27: 9469–9481, 2007.

Zurita P, Villa AE, de Ribaupierre Y, de Ribaupierre F, Rouiller EM. Changes of single unit activity in the cat's auditory thalamus and cortex associated to different anesthetic conditions. *Neurosci Res* 19: 303–316, 1994.